Validation of Anode Model for Voltage Drop Mitigation Studies

Mohamed I Hassan[1], Ayoola Brimmo[2], Rawa Ba Raheem[3], Tapan K Sahu[4], Mohamed Mahmoud[5], Vinko Potocnik[6]
1. Assistant Professor
2. Research Engineer,
Mechanical and Materials Engineering Department, Masdar Institute of Science and Technology, Abu Dhabi, UAE
3. Lead Engineer – Process Control, Reduction
4. Manager – Process Control & Improvement, Carbon and Port
5. Manager Technology Improvements – Technology Development & Transfer
6. Consultant
Emirates Global Aluminum (EGA) Jebel Ali (DUBAL), Dubai, UAE
Corresponding author: miali@masdar.ac.ae

Abstract

In aluminum smelters, the anode of a typical reduction cell has been widely reported as a location where significant amount of energy is wasted. These devices need optimization and a practical tool for this is the thermo-electro-mechanical (TEM) finite element model. In view of developing a computational tool fit for such optimization efforts, this study focuses on calibrating the contact stiffness factor (CSF) and on validating developed TEM models of the 4- and 8-flute anodes. Plant measurements of the anode stub to carbon (STC) and total (TVD) voltage drop, across the lifespan of the anode, were made for model validation. Calibration of the numerical model showed that CSF of 0.15 - 0.2 is adequate for the 8-flute anode while CSF of 0.5 is adequate for the 4-flute anode. Using these CSFs, results show that onsite measurements match the STC voltage drop and TVD, calculated by the TEM model. Overall, this article is an update on our finite element modeling of the aluminum-reduction cell anode.

Keywords: Aluminum reduction cell anode; anode model validation; anode voltage drop; contact stiffness factor.

1 Introduction

The anode of the aluminum-smelter has been recurrently singled out as a part of the reduction cell, which holds some potential for reducing energy consumption, if properly optimized [1,2,3,4,5,6,7,8]. As connections between the steel-stubs and the carbon blocks are made by pouring molten cast iron in the space between both materials, shrinkage of the cast iron connector (thimble) introduces imperfection to the stub-carbon contacts. In addition, the toe-in of the tripod stub [9] and suspension of the anode from the busbar [10], also contribute to the imperfection at the interface. From an electrical perspective, these imperfections denote an increased contact resistance and therefore, increased voltage drop and energy consumption of the anode.

Minimizing these imperfections is the ultimate aim of most studies in this line of research. The literature in this field can be summarized as early lab-scale experimental works focused on measuring the thimble-carbon contact voltage drop as a function of temperature and pressure [11,12] and later work focused on developing finite element models of the anode setup [10]. In between, some researchers attempted carrying out more experiments to calculate the voltage drop at these contacts as a function of stub size [8]. This was then followed up with computational models with the same stub-reduction strategy in view [9]. Overall, to adequately

simulate the anode physical operation, coupling of the thermal, electrical, and structural fields has proven to be the key for such models.

TEM models developed for the anode have shown a lot of promise; however, till date, these tools still have limitations. The typical drawbacks of the available anode models are:

(1) Inadequate modeling of the casting process,
(2) Use of wrong location for fixed constraint,
(3) Lack of transient analyses,
(4) Inadequately modeled thimble-carbon electric contact resistance,
(5) Excessive computational time and
(6) Lack of validation with plant measurements.

As such, the future should be directed at eliminating all these drawbacks by:

(1) Modeling the thimbles reference at its casting temperature to ensure adequate room temperature thimble-carbon air gaps are solved by the computational code,
(2) Applying the fixed constraint boundary at the top of the stub in order to adequately model the anode suspension from the busbar,
(3) Modeling the anode from the time it is newly inserted till when the carbon block is fully consumed and removed (end of life),
(4) Using deduced and validated relations to model the thimble-carbon contact voltage drop as a function of contact temperature and pressure, from our previous study [2],
(5) Applying an expedited and validated coupling computational technique [1,2] and
(6) Using plant anode voltage measurements to validate our models.

In our previous work [1], we considered the aforementioned drawbacks, but our efforts did not include complete model validations and transient considerations. As such, conclusions could not be drawn about the efficacy of the energy saving strategies assessed. Also, our results revealed strong dependence of the voltage drop results on the CSF, which highlighted the need for further calibration with plant measurements for quantitatively accurate results. This is an important consideration in anode modeling, which is most often completely overlooked. As mentioned earlier, the thimble-carbon interface is imperfect; hence, a mathematical formulation that allows for nodal interface separation is required to adequately model the contact behavior and hence electrical and thermal contact resistance. As such, the frictional contact formulations, which allow for nodal contact sliding, opening and closing, depending on the contact force, are befitting. However, these formulations are typically controlled by either the Pure Penalty or the Augmented Lagrangian model [13], which model the contacts as a hypothetical spring with the contact gap directly proportional to the contact pressure. The proportionality constant of this relation is the contact stiffness factor (CSF). The contact pressure and hence electrical contact pressure are dependent on CSF as such; the calculated voltage drop is dependent on the CSF utilized. The only way of knowing the correct CSF is by calibration with measurements; hence, calibration is a necessary step for the development of quantitatively accurate anode models [1] and this is also an important consideration in the present work.

Overall, this work reports the development, calibration and validation of a transient TEM finite element model of the aluminum reduction cell anode. The model formulation is based on our previously developed anode model [1], and calibration and validation are carried out using plant measurements on operating pots.

2 Mathematical Model

The domain and boundary conditions of the developed anode model is presented in Figure 1. The boundary conditions of Figure 1 are based on the beginning-of-life anode; however, we

model the anode from its beginning-of-life till the carbon block is fully consumed up to a practical limit of a few centimeters below the stub. To achieve this, the carbon block is modeled to be consumed by 1.8 cm per day, according to plant data. The thermal boundary conditions are: A temperature of 960 °C is applied from the bottom surface of the carbon block to about 15 cm of carbon height, which is based on the measured bath temperature and typical anode immersion depth. A current of 11 kA is applied on the top of the yoke distributed uniformly over the surface A; this corresponds to the pot current of 396 kA. Heat transfer coefficients of the un-immersed portion of the anode are based on Fortin et al [9] suggestions and our previous work [1]. The insulating effect of the anode cover is implicitly included in the model with an adiabatic boundary condition, i.e., no heat loss from the cover; this somewhat overestimates the anode temperature at the top and in the stub-carbon contact area. The anode setup is structurally constrained at the top of the steel yoke in order to take into account its suspension from the busbar. The 3.34 kN force applied at the bottom of the anode block is used to account for the buoyancy force acting on a beginning-of-life anode. As the anode life increases, the volume of the anode immersed in the bath somewhat decreases and so does the applied buoyancy force. Material properties of the anode assembly are based on sources used in our previous models [1].

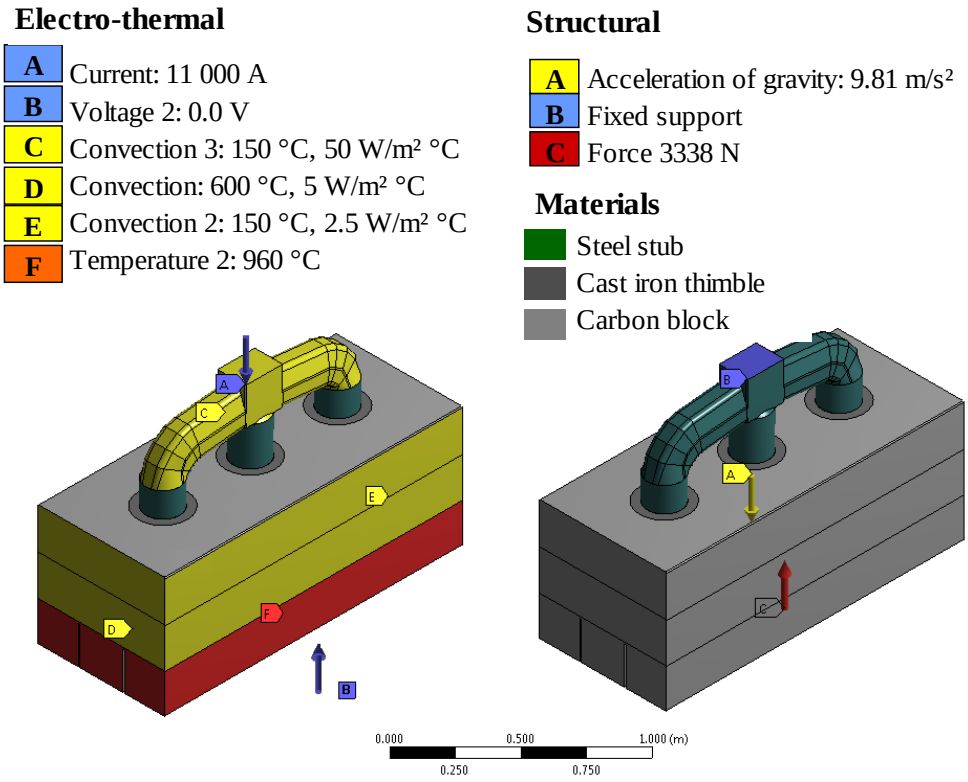

Figure 1. 3-D representation of the beginning-of-life anode boundary conditions.

To adequately model the initial air gap, the reference temperature for the thimble thermo-structural analysis is set at the casting temperature of 1 400 °C; this ensures that at ambient temperature, there is a gap at the thimble-carbon contact interface. The electrical resistances at these contacts are undoubtedly temperature and pressure dependent; hence, our deduced and validated correlations were adapted [1]. More details on the adapted mathematical formulation, computational techniques, and contact models can also be found in our previous publications [1,2].

Varying CSF from 0.1 - 0.7, we use the model to calculate the voltage profile of the anode setup. From this, we measure the anode stub-to-carbon (STC) voltage drop and anode total voltage drop (TVD) according to specifications from the plant measurements. This study was carried out as a function of time – from early-life anode to end-of-life anode – by consuming the carbon block and adjusting the buoyancy force appropriately. The bath temperature at the bottom of the carbon block is maintained at 15 cm immersion regardless of the total carbon height.

3 Plant Measurements

The measurements were carried out on DX pots in DUBAL Potline 8 since the model geometry was set up for these anodes. Pot current was: 400.3 kA during STC voltage drop measurements, 400.3 kA during 8-flute TVD measurements and 405.0 kA for 4-flute TVD measurements. For the analysis, these voltage drops were normalized to the model current of 396 kA (11 kA per anode).

3.1. Stub-to-carbon (STC) voltage drop

The stub-to-carbon voltage drop across ten operating anodes – five with eight flutes and five with four flutes – was monitored in the plant using voltage probes at positions V_2 and V_3 as shown in Figure 2. The measurements were standardized across all sampled anodes with 150 mm spacing between the probes V_2 to V_3. STC voltage drop measurements were made on the outer stub only; this may have contributed to the scatter of the results because it is possible that the current distribution between the three stubs was not uniform. The measurement interval was approximately 32 hours over the total anode life of about 27 days. The anodes selected for these measurements were thermally and electrically stable since the pots were in normal operation and not in early post star-up operation. Measurements from all the pots were collected and analyzed statistically to produce STC ($V_2 - V_3$) voltage drop trend across the anode life.

3.2. Total voltage drop (TVD)

As per standard practice in DUBAL, the total anode voltage drop was measured between the top of anode rod below the anode beam (V_0, not shown in Figure 2) and the bottom surface of the anode, V_4 (shown in Figure 2), which was at about 150 mm from the anode corner. The anode rod voltage drop was also measured, $V_0 - V_1$, and subtracted from $V_0 - V_4$ to obtain TVD, $V_1 - V_4$, as referred to in the model. The measurements were made in two measurement campaigns, one for 4-flute anode and one for 8-flute anode. The pots for TVD measurement were different than for STC measurement because they were made at different times. As per standard practice, all anodes in a selected pot were measured on the same day; only the anodes less than one day old (if any) were omitted. To access the bottom of each anode with a specially designed hook electrode, a hole was made at the corner of each anode pair, from which two adjacent anodes were measured. The individual anode voltage drops were plotted as a function of anode age and from a straight line fit, the anode voltage drop at mid age was calculated; this is referred to as the average voltage drop of all anodes. In this paper, the model TVD as a function of anode age is compared with the measured TVD and this is the most important part of the model validation. The measured voltage drops were normalized to the pot current of 396 kA (11 kA/anode) used in the model.

Model validation with TVD is more important than with STC voltage drop, since TVD is directly related to the pot energy consumption, whereas STC voltage drop is used only for quality control of thimble casting. However, STC does help validating the model around the stubs locally.

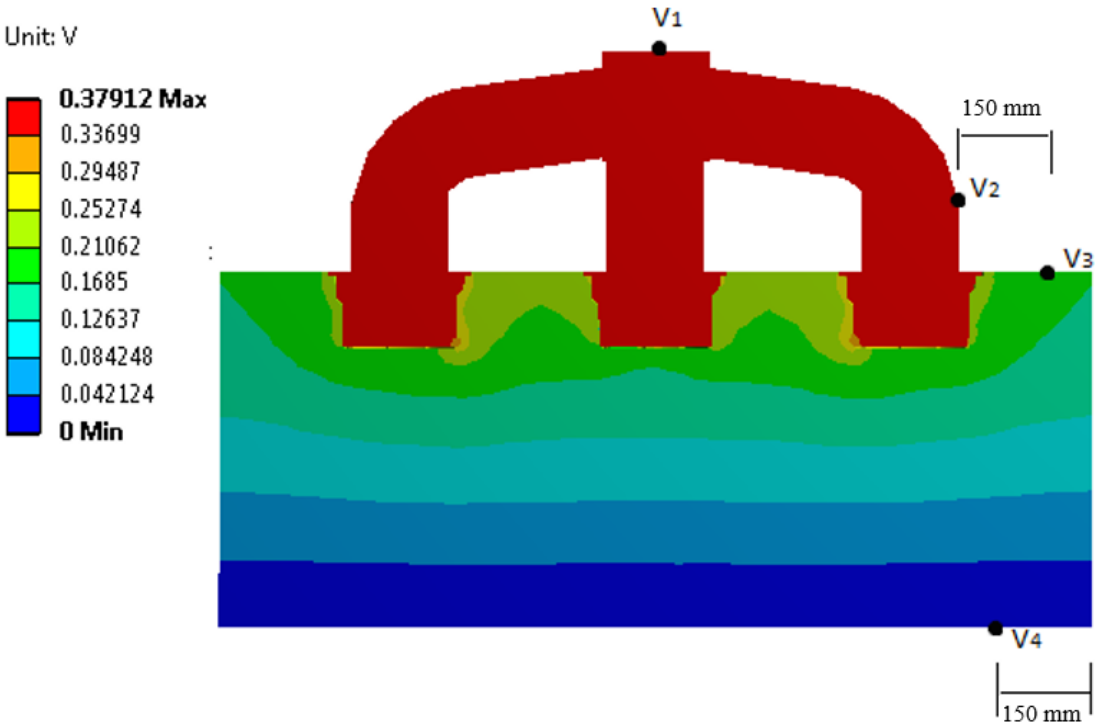

Figure 2. Voltage drop contour (8-flute anode) with position of probes for plant STC and TVD measurements.

4 Results

4.1. STC measurements

The raw STC measurements from the anodes with 8 flutes are shown in Figure 3 while that of the anodes with 4 flutes are shown in Figure 4. The general trend from both scatter plots is that the STC voltage drop reduces with cell life until about 15 - 20 days; after which STC voltage drops begin to slightly increase. However, this interpretation could be misleading as the STC measurements contain a lot of scatter; hence, a statistical analysis is required to retrieve a reliable trend. The average data are shown in Figure 5. There is a small difference between 8-flute and 4-flute design. Overall measured average STC voltage drop was 150 ± 15 mV for 8-flute anodes and 143 ± 21 mV for 4-flute anodes, an insignificant difference, considering the large standard deviations.

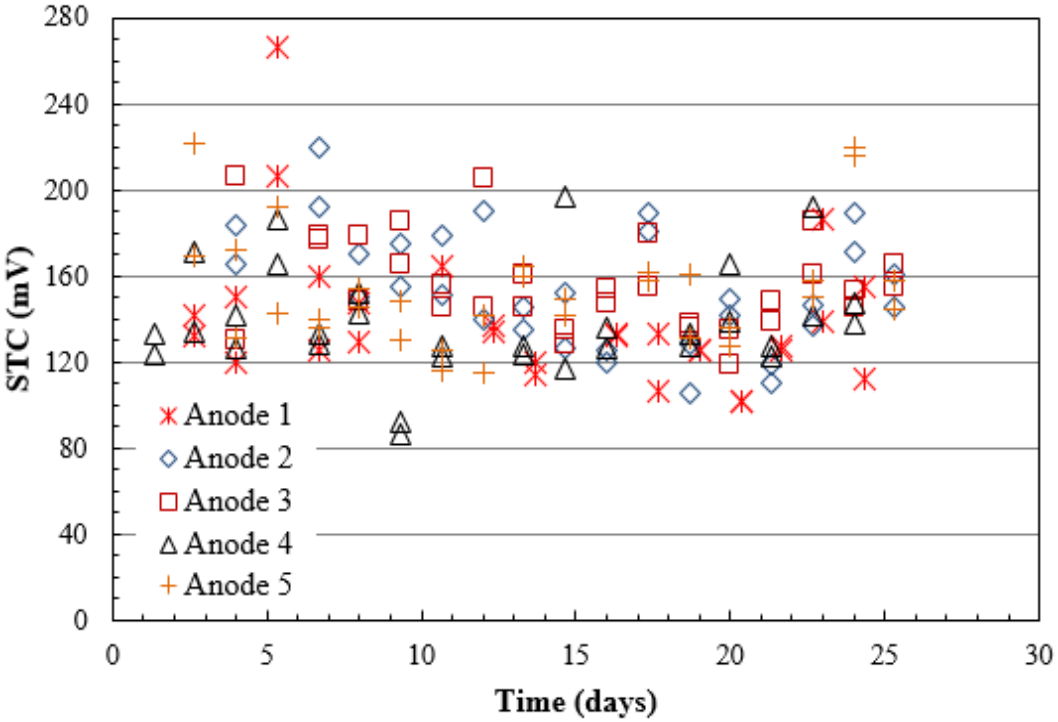

Figure 3. Raw STC measurements as a function of cell life (8-flute anode).

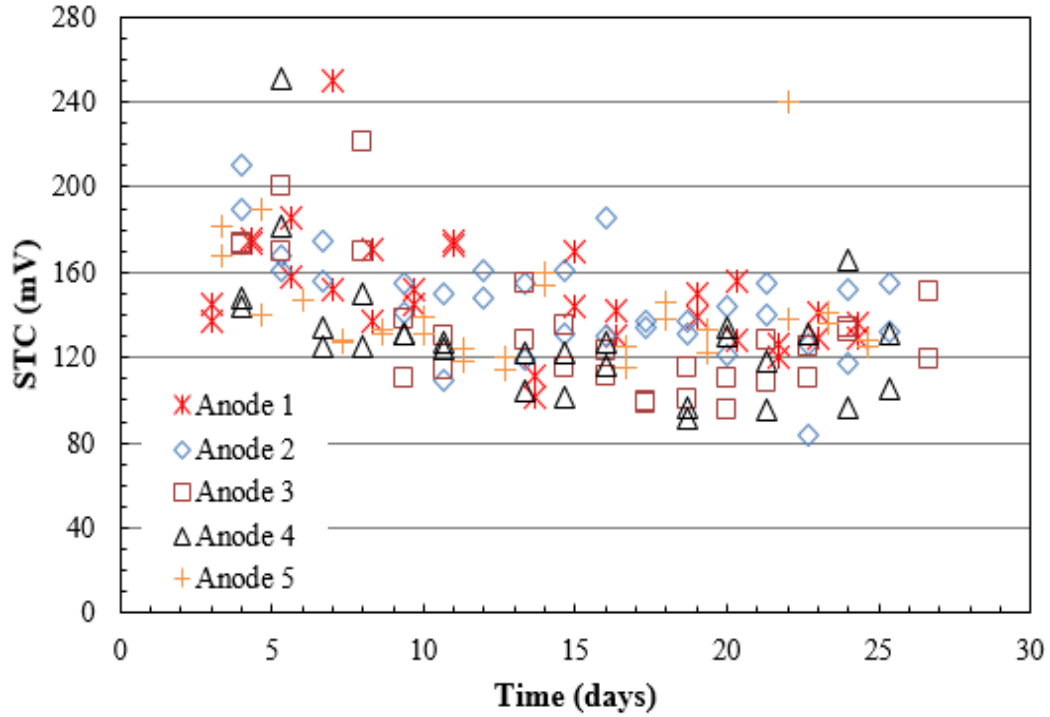

Figure 4. Raw STC measurements as a function of cell life (4-flute anode).

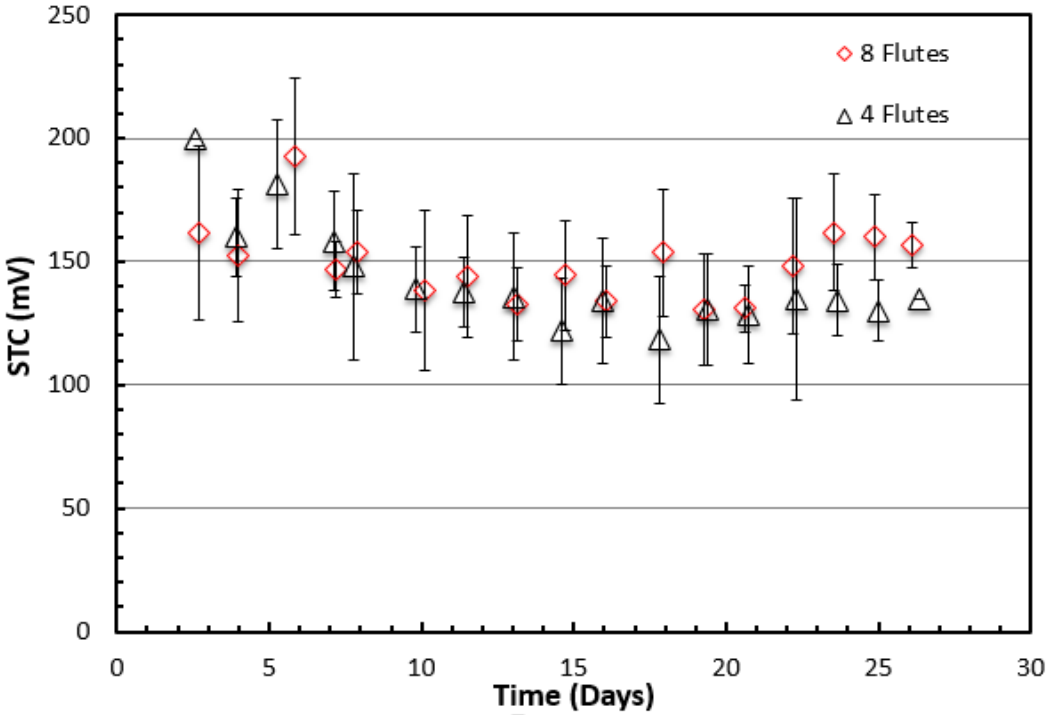

Figure 5. Average measured STC voltage drops as a function of cell life (4- and 8-flute anode).

4.2. Model validation for 8-flute anodes

To obtain voltage drop numerical calculations as a function of CSF, we changed the contact stiffness for each run of the model. Both STC and TVD voltage drop portrayed dependence on CSF, which is purely due to the contact formulation that calculates the contact pressure as a product of contact separation and CSF. Hence, for a given contact separation, an increase in CSF translates to an increased contact pressure, which in turn results in a reduction in electrical contact resistance. Figures 6 and 7 show the averaged STC and TVD measurements respectively – with error-bars indicating their standard deviation – in comparison to the numerically calculated voltage drop values, for the 8-flute anode. In Figure 6, the numerical results are presented for a CSF value of 0.2 as this value portrayed best fit with the measurements. From the figure, it can be seen that the measured STC voltage drops across the anode-life are fairly constant with slight increase after the anode age of 20 days. The model calculation also shows that STC voltage drop increases slightly with anode life and matches well with the plant measurements. The reason for this increase has not been found, since the contrary could be expected as the temperature of the anode and of the thimble-carbon contact increases, the contact pressure increases and lower contact voltage drop is expected.

Measured and numerically calculated TVD shown in Figure 7 agree well and both portray a reduction with anode life. TVD responds to carbon consumption, i.e., reduction of anode height and to the decrease of the thimble-carbon voltage drop for most of anode life. In practice, the competing processes, which tend to increase the TVD at the end of anode life is the decrease of anode length and width, an increase in STC and difficulty to distribute the current uniformly in a very thin anode butt. In spite of this, considering fairly large scatter of TVD measured data, a straight-line curve fit, showing monotonous TVD decrease, is a fair representation for comparison with the model, which also gives a straight line. CFS 1.5 (averaged from model calculations for CSF of 0.1 and 0.2) gives the best fit for TVD of 8-flute anodes.

The mid-life (age of 13.33 days) voltage drop of 8-flute anodes, representing the average of all anodes, is nearly the same in the model with CFS of 0.15 (361 mV) as measured (363 mV).

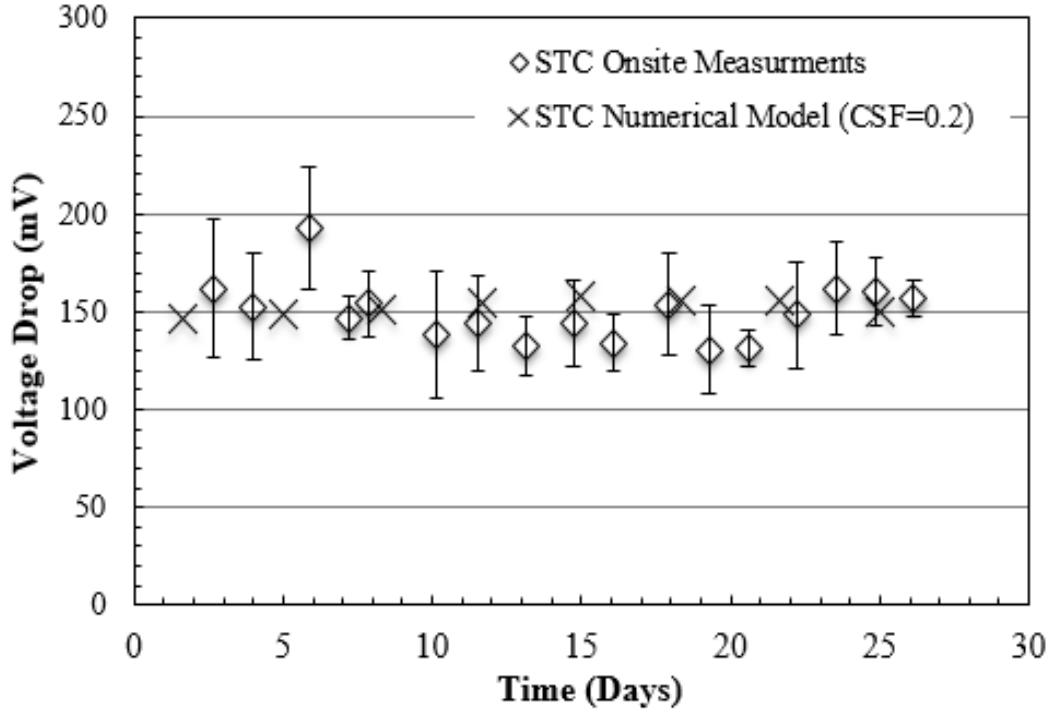

Figure 6. Comparison of measured and calculated STC voltage drop for the 8-flute anode.

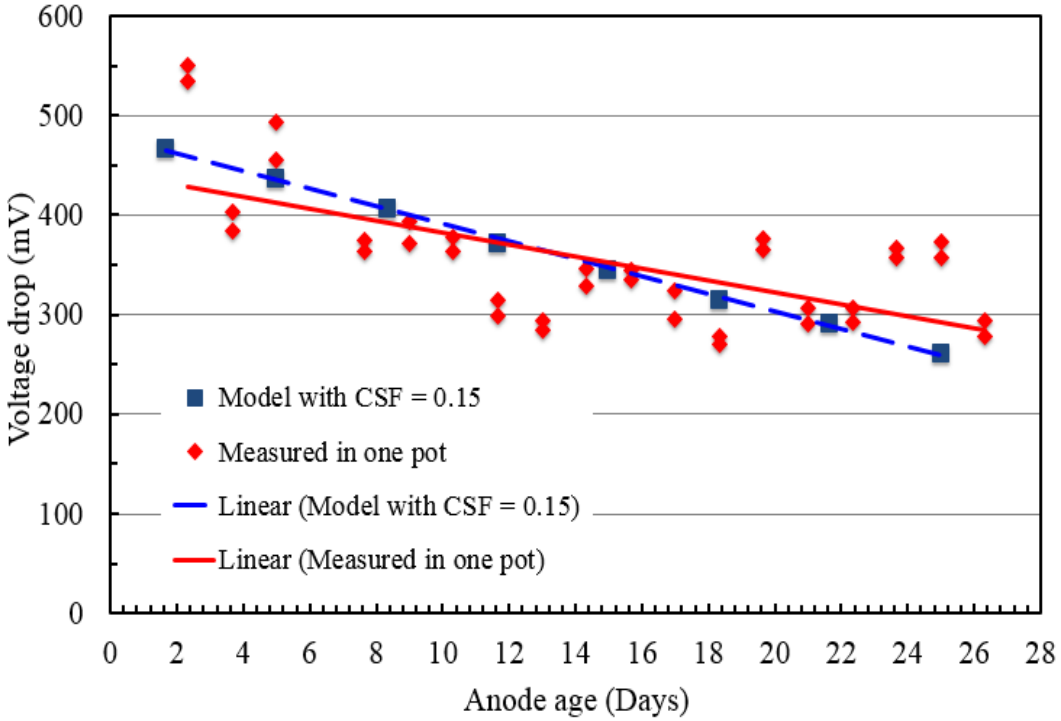

Figure 7. Total anode voltage drop in anodes with 8 flutes.

4.3. Model validation for 4-flute anodes

Figures 8 and 9 show the corresponding STC and TVD comparison for the 4-flute anode, respectively. STC measurements and numerically calculated results for 4-flute anode portray similar trends as those of the 8-flute anode. Best-fit CSF for this anode design was found to be 0.5. However, between the 12th and 22nd day, the numerically calculated STC values considerably overestimate the measurements. We believe this could be either due to measurement errors or a signal for re-calibrating the pressure and temperature dependent contact voltage drop, which was originally calibrated for the 8-flute anode.

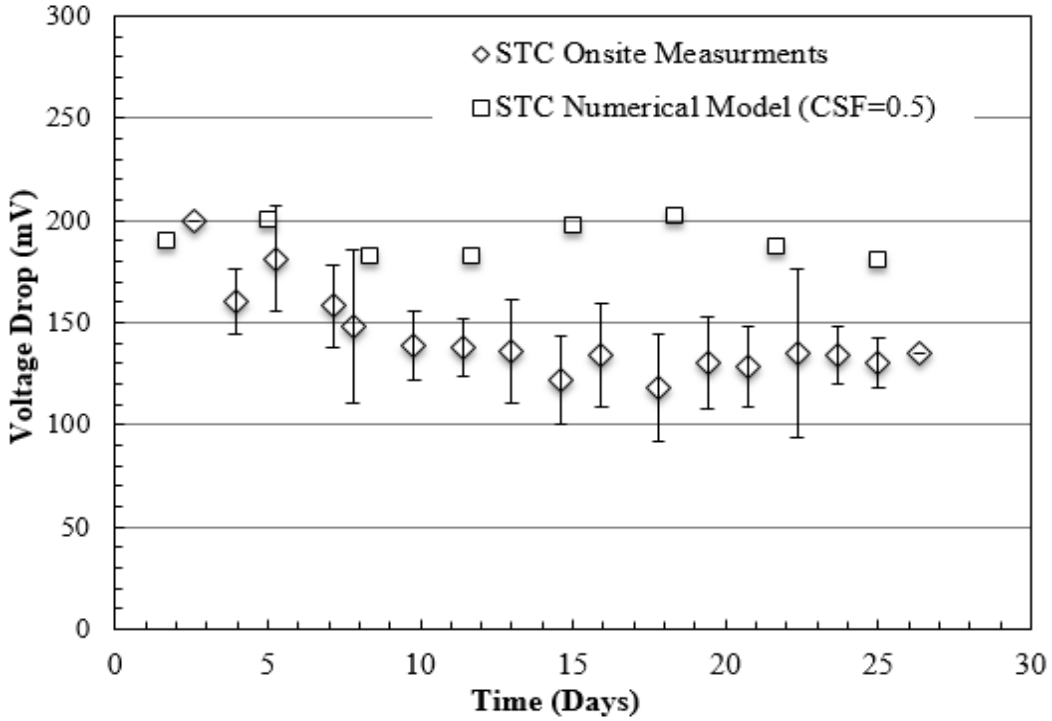

Figure 8. Comparison of experimental and calculated stub-to-carbon (STC) voltage drop for the 4-flute anode.

The anode total voltage drop (TVD) is shown in Figure 9. Considering fairly large scatter of the measured data, the modeled and the measured TVD agree very well as function of anode age. The somewhat higher measured TVD at the end of anode life in comparison to the model is at least in part due to the decrease of anode area, which is not taken into account in the model.

The mid-life (age of 13.33 days) TVD in the 4-flute anodes, representing the average of all anodes, is nearly the same in the model with CSF = 0.5 (380 mV) as measured (378 mV).

The CSF is different between the 4- and 8-flute anodes because of the different contact surface area and therefore different contact pressure between the thimble flutes and carbon.

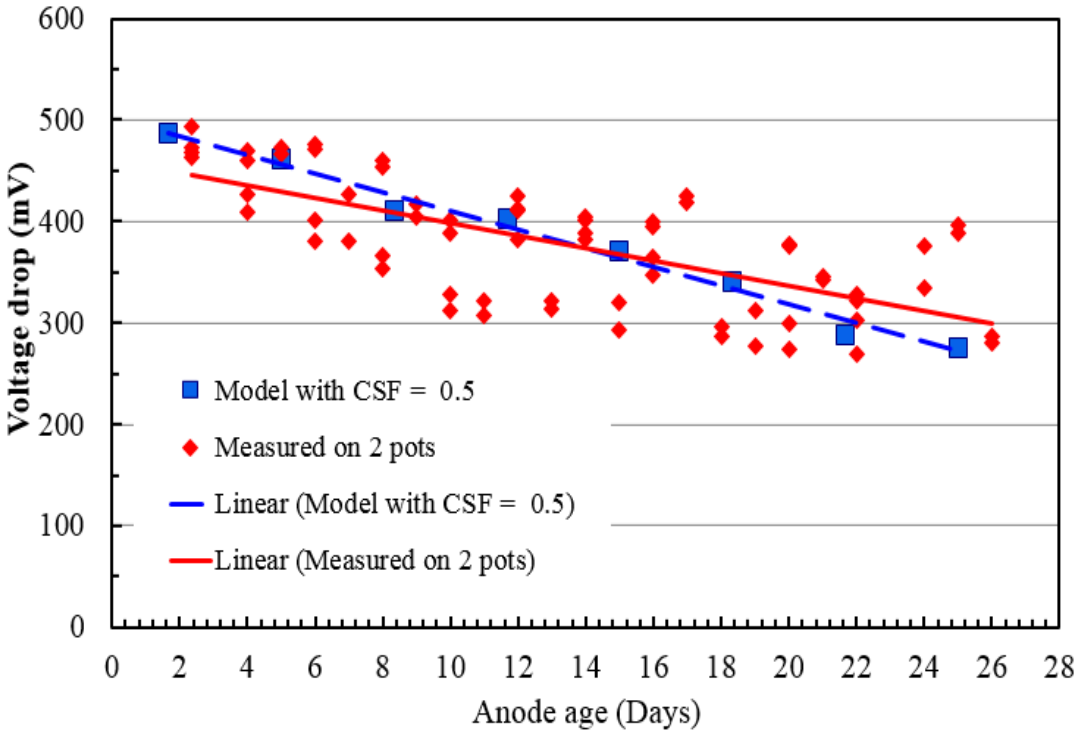

Figure 9. Total anode voltage drop in anodes with 4 flutes.

5 Conclusion

In this study, we have developed and validated a transient anode model of an aluminum-reduction cell, for the whole life of the anode. The contact stiffness factor (CFS) is used as an adjustable parameter for model validation with stub-to-carbon (STC) voltage drop and total voltage drop (TVD).The model validation shows that CSF in the range of 0.15 to 0.5 is adequate for the anode model, with CSF of 0.15 - 0.2 giving best fit for the 8-flute anode and CSF of 0.5 for the 4-flute anode. Numerically calculated STC voltage drop and TVD agree well with plant measurements.

6 Acknowledgement

We would like to thank Emirates Global Aluminum (EGA) for providing financial and technical support for this project. We would also like to thank all the members of staff at the Al Taweelah and Jebel Ali smelters who contributed with their efforts and useful discussions. Finally, we would like to particularly acknowledge the fruitful discussions with Jebel Ali cell modeling and design team for their very insightful comments regarding the operation and performance of their cells.

7 References

1. A. Brimmo et al, Anode design modeling for improved energy efficiency, *Proceedings of 33rd International ICSOBA Conference*, Dubai, United Arab Emirates, 29 November – 1 December 2015, *Travaux* 44, Paper AL24, 727-736.
2. A.T. Brimmo and M. I. Hassan, Modeling the electrical contact resistance at steel–carbon interfaces, *JOM*, vol. 68, no. 1, (2016), 49-58.
3. D. Molenaar, K. Ding, and A. Kapoor, Development of industrial benchmark finite element analysis model to study energy efficient electrical connections for primary aluminum

smelters, *Light Metals* 2011, 985-990.

4. D. Richard, M. Fafard, P. Clehry, R. Lacroix, and Y. Maltais, Aluminum reduction anode stub-hole design using weakly coupled thermo-electro-mechanical finite element models, *Finite Elements in Analysis and Design*, vol. 37, (2001), 287-304.
5. D. Richard et al, Challenges in the stub hole optimization of cast-iron rodded anodes, *Light Metals* 2009, 1055-1059.
6. M. Dupuis, Development and application of an ANSYS based thermo-electro-mechanical anode stub hole design tool, *Light Metals* 2009, 433-438.
8. S. Wilkening and J. Cote, Problems of the stub-anode connection, *Light Metals* 2007, 534-542.
7. M. Sorlie and H. Gran, Cathode collector bar-to-carbon contact resistance, *Light Metals* 1992, 779-787.
9. H. Fortin, N. Kandev, and M. Fafard, FEM analysis of voltage drop in the anode connector induced by steel stub diameter reduction, *Finite Elements in Analysis and Design*, vol. 52, (2012), 71–82.
10. D.R. Gunasegaram and D. Molenaar, Towards improved energy efficiency in the electrical connections of Hall-Heroult cells through finite element analysis (FEA) modelling, *Journal of Cleaner Production*, vol. 93, (2015), 174-192.
11. D.G. Brooks and V.L. Bullough, Factors in the design of reduction cell anodes, *Light Metals* 1984, 961-976.
12. P.J. Rhedey and L. Castonguay, Effects of carbonaceous rodding mix formulation on steel-carbon contact resistance, *Light Metals* 1985, 1089-1105.
13. J.C. Simo and T.A. Laursen, An augmented Lagrangian treatment of contact problems involving friction, *Computer and Structures*, vol. 42, no. 1, (1992), 97-116.